Rare Metal Materials and Engineering
Volume 47, Issue 4, April 2018
Online English edition of the Chinese language journal

Available online at www.sciencedirect.com
ScienceDirect

Cite this article as: Rare Metal Materials and Engineering, 2018, 47(4): 1064-1068.

ARTICLE

Effect of Texture on the Performance of Mg-air Battery Based on Rolled Mg-3Al-1Zn Alloy Sheet

Zhao Yanchun[1,2], Huang Guangsheng[1,2,3], Zhang Cheng[1,2], Chen Lin[1,2], Han Ting-zhuang[1,2], Pan Fusheng[1,2,3]

[1] College of Materials Science and Engineering, Chongqing University, Chongqing 400044, China; [2] National Engineering Research Center for Magnesium Alloys, Chongqing University, Chongqing 400044, China; [3] State Key Laboratory of Mechanical Transmission, Chongqing University, Chongqing 400044, China

Abstract: Commercial rolled Mg-3Al-1Zn (AZ31) alloy sheet was used as the experimental material, an Mg-air battery based on its rolling surface (RS) and cross-section surface (CS) were both prepared to study the effect of texture on the performance of Mg-air battery. And the experimental samples had a similar surface roughness to practical application. The impedance spectroscopy (EIS) was used to investigate the electrochemical behavior of the samples. The results show that CS surface has a higher corrosion resistance compared with the RS surface. The battery performance was studied by constant current discharge test, and the results show that the Mg-air battery based on the CS surface anode has higher anode efficiency (71.3%) compared with the Mg-air battery based on the RS surface anode (65.7%). The surface morphologies of the magnesium alloy anodes substrate after discharged for 24 h were observed by scanning electron microscope. The RS anode exhibits a magnesium alloy anode substrate with more holes and gullies, which may contribute to its lower anode efficiency. Thus, the CS anode dominated by $(10\bar{1}0)$, $(11\bar{2}0)$ and $(10\bar{1}1)$ orientated grains is more suitable to use on Mg-air battery.

Key words: AZ31 Mg alloy; texture; corrosion resistance; Mg-air battery; anode efficiency

Owing to the growing concern on the energy crisis, more researchers began to study about new energy[1-5]. Mg-air battery is considered as a promising power source to replace traditional energy because of its high specific energy, light weight and no pollution[2,3,6,7]. However, Magnesium alloy has a high self-corrosion rate in neutral salt solution. The further development and commercial exploitation of Mg-air battery was significantly restricted due to its low anode efficiency.

Considerable efforts have been devoted to improve the anode efficiency of Mg-air battery. For example, Ma et al[6] investigated the corrosion and discharge behavior of Mg, AZ31 and Mg-Li-Al-Ce in 3.5 wt% NaCl solution. They found that using Mg-Li-Al-Ce as anode could improve the performance of Mg-air battery, which reduces the capacity loss and improves the anode efficiency. Yuan et al[8] modified the electrochemical performance of Mg-3Al by Ga, In and Sn. The results showed AI31 behaves good comprehensive properties; the battery based on AI31 anode possesses the capacity density (1382 $mA{\cdot}h{\cdot}g^{-1}$) and power density (18.5 $mW{\cdot}cm^{-2}$). As is well known, deformation texture can be easily generated on Mg alloy and adjusted by various processing methods[9-12]. Song et al[13] found that crystallographic orientation has a significant effect on the corrosion behavior and electrochemical activity of AZ31 Mg alloy. Its rolling surface dominated by crystallographic plane (0001) exhibits a more negative electrochemical activity and a faster corrosion rate. Xin et al[14] investigated the influence of the texture on corrosion rate of AZ31 Mg alloy in 3.5 wt% NaCl. They found that the corrosion rate of AZ31 dramatically increased as the (0001) texture intensity decreased and the

Received date: April 25, 2017
Foundation item: National Natural Science Foundation of China (51531002); Demonstrative Project of Chongqing Science and Technology Commission (CSCT2014FAZKTJCSF50004); Fundamental Research Funds for the Central Universities (CDJZR14130009)
Corresponding author: Huang Guangsheng, Ph. D., Professor, College of Materials Science and Engineering, Chongqing University, Chongqing 400044, P. R. China, Tel: 0086-23-65112239, E-mail: gshuang@cqu.edu.cn

$(10\bar{1}0)/(11\bar{2}0)$ texture intensity increased. These studies recover that crystallographic texture has a prodigious effect on the electrochemical performance of Mg alloy, which may also affect the performance of Mg-air battery. However, the previous studies only investigated the influence of texture on the electrochemical performance of Mg alloy with an ultra-smooth surface. And how texture influences the corrosion behavior of magnesium alloy with a relatively rough surface is not well understood. In practical application, Mg alloy sheet was generally polished by abrasive belt grinding. Most commercially used Mg alloy has a surface with higher roughness compared with the test samples reported in the previous two studies[13,14]. On the other hand, the effect of texture on the performance of Mg-air battery has seldom been reported.

Hence, in the present study, an Mg-air battery based on AZ31 alloy with different grain orientations was prepared. The surface roughness of the test samples is similar to that of practical application. The battery performance was studied by X-ray diffraction patterns, electrochemical impedance spectroscopy, constant current discharge test and scanning electron microscopy.

1 Experiment

Commercial rolled AZ31 Mg alloy sheet was used as the experimental material, which was cut along its rolling surface and cross-section surface (Fig.1). Here, RD, ND and TD represent the rolling direction, the normal direction and the transverse direction of the rolled sheet, respectively. For the EIS test, the specimens were cut into 20 mm×20 mm×2 mm and ground with 400-grit SiC paper along the TD direction subsequently. In industrial production of Mg alloy sheet at present, the surface of sheet was ground with abrasive belt ultimately which is similar to that used in the current experiment. The samples for the discharge performance test were also prepared by fine grinding the original specimen with a dimension of 20 mm×30 mm×1.8 mm to a final thickness of 1.6 mm with 400-grit SiC paper along TD direction. The optical microstructures of the samples were examined by optical microscopy. The solutions were prepared using Analar grade reagents and triply distilled water. All experiments were carried out at 25±2 °C in non-deaerated solutions and repeated for three times.

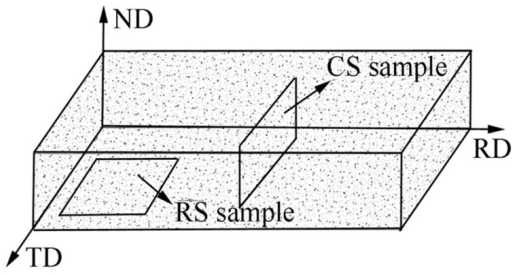

Fig.1 Schematic illustration of sample preparation

The electrochemical impedance spectra (EIS) measurements were performed for approximately 30 min after immersion of the sample to ensure the stability of the system. A three-electrode electrochemical cell was designed, the working electrode was the RS and CS anodes, the counter electrode was platinum electrode and the reference electrode was saturated calomel electrode. The measurements of the electrochemical impedance spectra (0.1~10^5 Hz, 5 mV, at open circuit potential) were performed in neutral 3.5 wt% NaCl solution with a PARSTAT 2273 system. A Zview software was then used for fitting the EIS results.

An Mg-air battery consisting of anode, cathode and electrolyte was prepared where the anodes were RS and CS samples, the cathode was air anode with MnO_2 catalyst and the electrolyte was neutral 3.5 wt% NaCl solution. The constant current discharge test was accomplished at a current density of 10 mA·cm^{-2} using a battery testing system (BTS-MPTS, China). The mass of consumed Mg was used to calculate the anodic efficiencies of the batteries. The anodic efficiencies were calculated using Eq. (1) [15,16]:

$$\text{Anodic efficiency}\ (\%)=(i\times A\times t\times M_a)/(2F\times W_c)\times 100\% \quad (1)$$

where i is the current density (A·cm^{-2}), t is the total discharge time (h), F is the Faraday constant (96 485 C·mol^{-1}), A is the surface area (cm^2), M_a is the atomic mass (g·mol^{-1}) of the specimens and W_c is the mass of consumed Mg alloys.

The texture components of the RS and CS samples were confirmed by X-ray diffraction (XRD) patterns using a Rigaku-DMax/2500PC (Japan). The product films on the magnesium alloy substrate after discharged for 24 h were cleaned in 200 g/L CrO_3 + 10 g/L $AgNO_3$ solution, and then the surface morphologies of the magnesium alloy substrate were observed using a TESCAN VEGA-3 LMH scanning electron microscope (SEM).

2 Results and Discussion

2.1 Electrochemical behavior analysis

Fig.2 shows the optical microscopic images of the RS and CS surfaces. It can be found that the RS and CS surface exhibit an almost identical grain size distribution, with an average grain size of 25.0 and 25.1 μm, respectively. Thus, the grain size difference is not responsible for the corrosion and discharge performance difference in this study. Fig.3 displays the EIS plots of the RS and CS surfaces. Both of the plots consist of a capacitive loop at high frequency and a relatively-small capacitive loop at low frequency. The high frequency capacitive loop is resulted from charge transfer and a film effect, and the low frequency capacitive loop is resulted from a mass transport relaxation in the surface layer[17,18]. The equivalent circuits of the EIS plots are shown in Fig.4. A constant-phase element representing a shift from an ideal capacitor was used instead of the capacitance itself, for

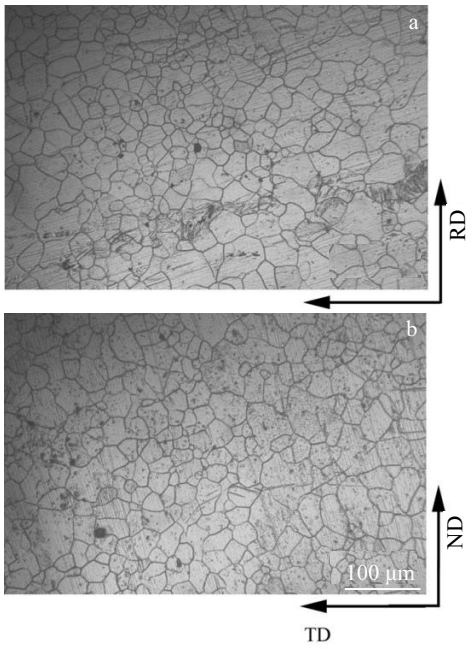

Fig.2 Optical microscopic images of RS sample (a) and CS sample (b)

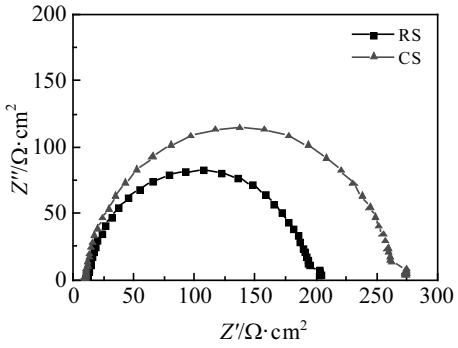

Fig.3 EIS plots of the AZ31 samples measured in neutral 3.5 wt% NaCl solution

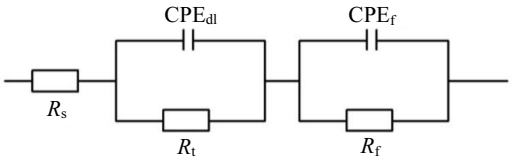

Fig.4 Equivalent circuits of the EIS plots in Fig.3

simplicity. In Fig.4, R_s represents the solution resistance, CPE_{dl} represents the electric double layer capacity, R_t represents the charge transfer resistance, CPE_f represents the film capacity and R_f represents the film resistance. The EIS fitting results are listed in Table 1. The reciprocal of R_t reflects the corrosion resistance of the RS and CS samples, which is 180.5 and 242.4 $\Omega\cdot cm^2$, respectively. The results demonstrate that the CS surface has a higher corrosion resistance compared with the RS surface.

However, the RS surface has a higher corrosion resistance than the CS surface according to the reported studies[13,14], which is opposite to the result in this study. The reasons are as follows. Fig.5 shows the texture components of the samples. The RS surface mainly consists of (0001) orientated grains, and the CS surface mainly consists of $(10\bar{1}0)$, $(11\bar{2}0)$ and $(10\bar{1}1)$ orientated grains instead. Thus, on an ultra-smooth surface similar to the reported studies[13,14], the RS surface mainly consists of crystallographic planes (0001) and the CS surface mainly consists of crystallographic planes $(10\bar{1}0)$, $(11\bar{2}0)$ and $(10\bar{1}1)$. In this study, the surfaces of all the samples are covered over by small gullies approximately parallel to the RS surface, which can be seen from the SEM photographs in Fig.6. Thus, the crystallographic planes exposed on the material surface change dramatically. The RS surface mainly consists of cylindrical planes and pyramidal planes, and the CS surface mainly consists of basal planes and pyramidal planes. That is, the crystallographic planes on the alloy surface in this study has a great difference with that exposed on a ultra-smooth surface similar to the reported studies[13,14] in rolled Mg alloy sheet.

As is well known, crystallographic planes (0001) has the biggest surface atomic density in Mg alloy, and a closed packed plane has a low surface energy. The surface energy for Mg (0001), $(10\bar{1}0)$ and $(11\bar{2}0)$ surface is 1.808, 1.868, and 2.156 eV/nm^2, respectively. The metal with a low surface energy has a high corrosion resistance[19,20]. According to Song et al[13], the theoretical dissolution rates of crystallographic planes $(10\bar{1}0)$ and $(11\bar{2}0)$ are 18~20 times higher than that of the crystallographic planes (0001). Consequently, the CS surface has a higher corrosion resistance than the RS surface.

2.2 Battery performance

Fig.7 shows the discharge behavior of the Mg-air battery with the RS and CS anodes. The two batteries show a similar discharge voltage. However, the CS battery has a higher anode efficiency (71.3%) compared with the RS battery (65.7%).

In the preliminary stage, the surfaces of the magnesium alloy substrates are covered over by small gullies produced during the sample preparation course. Owing to the discrepancy of the crystallographic planes exposed on the surface of the magnesium alloy substrate, the CS sample has a higher charge

Table 1 EIS fitting results of the AZ31 samples measured in neutral 3.5 wt% NaCl solution

Samples	$R_s/\Omega\cdot cm^2$	CPE_{dl}-T/$\mu F\cdot cm^{-2}$	CPE_{dl}-P/n_{dl}	$R_t/\Omega\cdot cm^2$	$CPE_f/\mu F\cdot cm^{-2}$	CPE_f-P/n_f	$R_f/\Omega\cdot cm^2$
RS	9.92	40.83	0.97	180.5	5859	0.49	31.34
CS	9.75	27.75	0.94	242.4	10 620	0.99	11.02

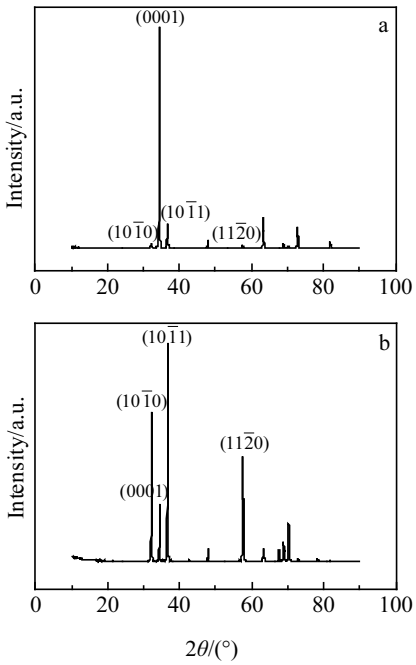

Fig.5 XRD patterns of RS surface (a) and CS surface (b)

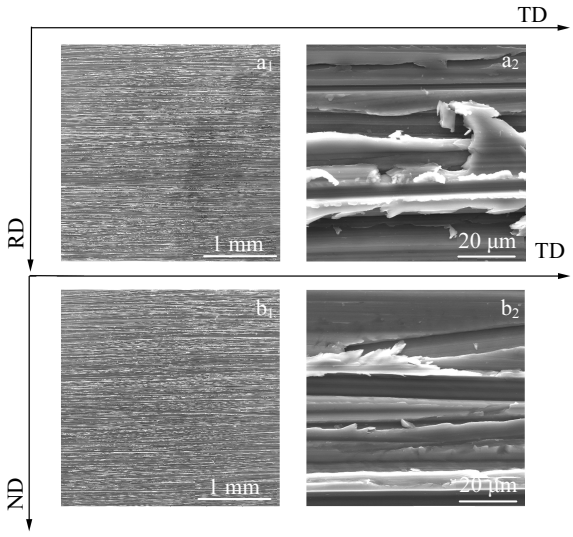

Fig.6 SEM micrographs of RS surface (a_1, a_2) and CS surface (b_1, b_2) ground with 400-grit SiC paper along TD direction

transfer resistance according to the analysis above. So, the CS battery has a slower corrosion rate.

Subsequently, the gullies on the magnesium alloy substrate surface produced during the sample preparation course are dissolved gradually. Fig.8 shows the surface morphologies of the magnesium alloy substrates after discharged for 24 h. The magnesium alloy substrates still show a surface with a high surface roughness, which may be caused by the local corrosion and discharge performance of the Mg anodes. On

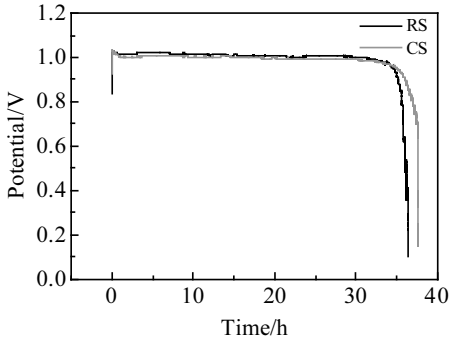

Fig.7 Discharge curves of the Mg-air battery at a current density of 10 mA·cm^{-2}

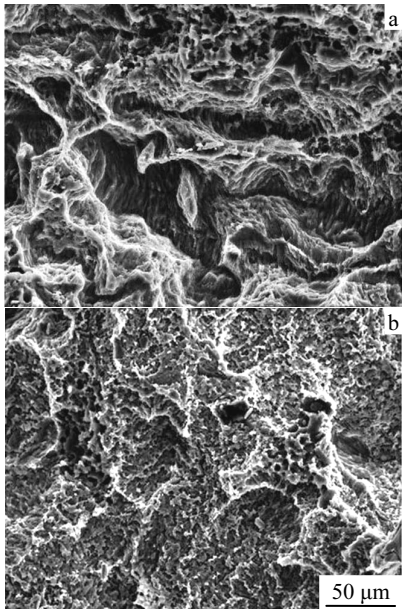

Fig.8 Surface morphologies of Mg alloy substrates after discharge for 24 h at a current density of 10 mA·cm^{-2}: (a) RS sample and (b) CS sample

the other hand, the RS anode has a high roughness magnesium alloy substrate surface, which may give rise to the lower specific discharge capacity of the RS battery. Because of the strong (0001) basal texture of Mg alloy, the *c*-axis of most grains in Mg alloy is perpendicular to the RS surface. However, the *c*-axis of a small number of grains is parallel to the RS surface, and the crystallographic planes (10$\bar{1}$0) or (11$\bar{2}$0) of these grains are approximately parallel to the RS surface. Crystallographic planes (10$\bar{1}$0) and (11$\bar{2}$0) have lower corrosion resistant than crystallographic planes (0001) in Mg alloy. Thus, the RS anode has a faster corrosion and discharge rate parallel to the normal direction in these areas, which gradually evolves into small holes or gaps. A small surface parallel to the RS surface is also formed in the holes and gaps, which mainly consists of crystallographic planes

(0001) with low corrosion resistance. The corrosion rate of the RS anode in the holes and gaps is further accelerated owing to the increased negative difference effect. On the other hand, the portal of the holes and gaps is gradually blocked by the corrosion and discharge product. Thus, the discharge process can hardly take place in the holes and gaps, which leads to the lower anode efficiency of the RS battery. As a result, the CS battery has a higher anode efficiency (71.3%) compared with that of the RS battery (65.7%).

3 Conclusions

1) The crystallographic planes on a relatively rough surface similar to practical application has a great difference with that exposed on a ultra-smooth surface in rolled Mg alloy sheet. Thus, the CS surface shows a better corrosion resistance compared with the RS surface which is opposite to that of the Mg alloys with an ultra-smooth surface.

2) The CS battery has a higher anode efficiency (71.3%) compared with the RS battery (65.7%). So the CS surface dominated by $(10\bar{1}0)$, $(11\bar{2}0)$ and $(10\bar{1}1)$ orientated grains is more suitable to use on Mg-air battery.

References

1 Virkar A V, Tao G. *International Journal of Hydrogen Energy*[J], 2015, 40(16): 5561

2 Blurton K F, Sammells A F. *Journal of Power Sources*[J], 1979, 4(4): 263

3 Peng B, Chen J. *Coordination Chemistry Reviews*[J], 2009, 253(23-24): 2805

4 Shangguan E B, Wang J L, Li J *et al*. *International Journal of Hydrogen Energy*[J], 2013, 38(25): 10 616

5 Obara S, Morizane Y, Morel J. *International Journal of Hydrogen Energy*[J], 2013, 38(21): 8888

6 Ma Y B, Li N, Li D Y *et al*. *Journal of Power Sources*[J], 2011, 196(4): 2346

7 Li W Y, Li C S, Zhou C Y *et al*. *Angewandte Chemie*[J], 2006, 118(36): 6155

8 Yuan S Q, Lu H M, Sun Z G *et al*. *Journal of The Electrochemical Society*[J], 2016, 163(7): A1181

9 Zhang H, Yan Y, Fan J F *et al*. *Materials Science and Engineering A*[J], 2014, 618: 540

10 Choi S H, Shin E J, Seong B S. *Acta Materialia*[J], 2007, 55(12): 4181

11 Yi S B, Davies C H J, Brokmeier H G *et al*. *Acta Materialia*[J], 2006, 54(2): 549

12 Li S Q, Tang W N, Chen R S *et al*. *Journal of Magnesium and Alloys*[J], 2014, 2(4): 287

13 Song G L, Mishra R, Xu Z Q. *Electrochemistry Communications*[J], 2010, 12(8): 1009

14 Xin R L, Li B, Li L *et al*. *Materials & Design*[J], 2011, 32(8-9): 4548

15 Cao D X, Wu L, Sun Y *et al*. *Journal of Power Sources*[J], 2008, 177(2): 624

16 Cao D X, Cao X, Wang G L *et al*. *Journal of Solid State Electrochemistry*[J], 2010, 14(5): 851

17 Chang J W, Guo X W, Fu P H *et al*. *Electrochimica Acta*[J], 2007, 52(9): 3160

18 Baril G, Blanc C, Pébère N. *Journal of the Electrochemical Society*[J], 2001, 148(12): B489

19 Abayarathna D, Hale E B, O'Keefe T J *et al*. *Corrosion Science*[J], 1991, 32(7): 755

20 König U, Davepon B. *Electrochimica Acta*[J], 2001, 47(1-2): 149

织构对基于 Mg-3Al-1Zn 合金的镁空气电池性能的影响

赵炎春[1,2]，黄光胜[1,2,3]，张　诚[1,2]，陈　琳[1,2]，韩廷状[1,2]，潘复生[1,2,3]

(1. 重庆大学 材料科学与工程学院，重庆 400044)

(2. 重庆大学 国家镁合金材料工程技术研究中心，重庆 400044)

(3. 重庆大学 机械传动国家重点实验室，重庆 400044)

摘　要：为了研究织构对镁空气电池性能的影响，以商用 AZ31 镁合金板材为实验材料，分别制备了基于板材轧面和截面的镁空气电池。所用实验材料的表面粗糙度与实际应用中镁合金板材的表面粗糙度相似。通过电化学阻抗谱研究了试样的电化学性能，结果表明截面比轧面更耐腐蚀。通过恒流放电测试研究了电池的放电性能，结果表明基于截面阳极的镁空气电池和基于轧面阳极的镁空气电池相比具有更高的阳极效率（2 种电池的阳极效率分别为 71.3%和 65.7%）。放电 24 h 之后，通过扫描电子显微镜研究了镁合金阳极基体的表面形貌。轧面阳极显示出一个具有更多孔洞和沟壑的阳极表面，这可能是导致它具有低阳极利用率的原因。因此，被$(10\bar{1}0)$、 $(11\bar{2}0)$ 和$(10\bar{1}1)$取向晶粒所主导的截面阳极更适合运用于镁空气电池。

关键词：AZ31 镁合金；织构；耐腐蚀性能；镁空气电池；阳极效率

作者简介：赵炎春，男，1988 年生，博士，重庆大学材料科学与工程学院，重庆 400044，E-mail: 492980897@qq.com